

Improving Visual Relation Detection using Depth Maps

Sahand Sharifzadeh¹, Sina Moayed Baharlou^{2*}, Max Berrendorf^{1*}, Rajat Koner¹
Volker Tresp^{1,3}

¹Ludwig Maximilian University, Munich, Germany

²Sapienza University, Rome, Italy

³Siemens AG, Munich, Germany

{sharifzadeh, berrendorf, koner}@dbs.ifi.lmu.de, baharlou@dis.uniroma1.it, volker.tresp@siemens.com

Abstract

State-of-the-art visual relation detection methods mostly rely on object information extracted from RGB images such as predicted class probabilities, 2D bounding boxes and feature maps. Depth maps can additionally provide valuable information on object relations, e.g. helping to detect not only spatial relations, such as *standing behind*, but also non-spatial relations, such as *holding*. In this work, we study the effect of using different object information with a focus on depth maps. To enable this study, we release a new synthetic dataset of depth maps, *VG-Depth*, as an extension to Visual Genome (VG). We also note that given the highly imbalanced distribution of relations in VG, typical evaluation metrics for visual relation detection cannot reveal improvements of under-represented relations. To address this problem, we propose using an additional metric, calling it *Macro Recall@K*, and demonstrate its remarkable performance on VG. Finally, our experiments confirm that by effective utilization of depth maps within a simple, yet competitive framework, the performance of visual relation detection can be significantly improved.

1 Introduction

In the last years, visual relation detection, i.e. detection of relations from images in the form of (*subject, predicate, object*), has gained a lot of interest. One reason is that understanding relations between entities can play an important role in decision making. For example, detecting whether a man is *on* a bike or *next to* a bike is a crucial challenge in autonomous driving. State-of-the-art works in this area utilize information of objects in the scene such as class labels, bounding boxes and RGB features. Depth maps can additionally provide valuable information about an object's relations as they provide the objects' distance from the camera. This information can help to distinguish between many relations such as *behind*, *in front of* and even improve detection in situations where the objects are nearby such as *covered in*. In this work we aim



Figure 1: An image from the Visual Genome dataset showing several men sitting next to each other and the corresponding generated depth map. Bright colors indicate a larger distance to the camera. Knowing the depth of, e.g., the individuals, the house and the car, plays an important role in detecting relations such as *next to* and *behind*.

to study the effect of using these different object information with a focus on depth maps.

Unfortunately, most available datasets, specifically the ones with relational annotations such as Visual Relation Detection (VRD) [Lu *et al.*, 2016] and Visual Genome (VG) [Krishna *et al.*, 2017], lack depth maps since their acquisition is a cumbersome task requiring specialized hardware. We tackle this issue by synthetically generating the corresponding depth maps from 2D images of Visual Genome. The availability of large corpora of RGB-D pairs, e.g. NYU-Depth-v2 [Nathan Silberman and Fergus, 2012] dataset enables us to learn the mapping between any RGB image to its corresponding depth map using a fully convolutional neural network. Applying this network to the images from VG, generates their corresponding depth maps (e.g. Figure 1). We release these depth maps as a dataset extending VG, calling it *VG-Depth*¹. The object information extracted from depth maps and RGB images, i.e. class labels, location vectors, RGB and depth features, are the basis for relation detection in our simple yet effected framework.

We note that the typically employed Recall@K metric, which we call Micro Recall@K, cannot properly reveal the improvements of under-represented relations in highly imbalanced datasets such as VG. This might be an issue in applications such as autonomous driving where it is important to ensure that the model is capable of predicting also important but less represented predicates such as *walking on* (648 in VG test set) and not just *wearing* (20,148 in VG test set). We address this issue by proposing to employ *Macro Recall@K*, where

* Authors contributed equally.

¹This dataset and our framework will be made publicly available.

we compute the mean over Micro Recall@K per predicate, thereby eliminating the effect that over-represented classes have in Micro Recall@K setting.

In summary, our contributions are as follows:

1. We perform an extensive study on the effect of using different sources of object information in visual relation detection. We show in our empirical evaluations using the VG dataset, that our model can outperform competing methods by a margin of up to 8% points, even those using external language sources or contextualization.
2. We release a new synthetic dataset *VG-Depth*, to compensate for the lack of depth maps in Visual Genome.
3. We propose *Macro Recall@K* as a competitive metric for evaluating the visual relation detection performance in highly imbalanced datasets such as Visual Genome.

2 Related Works

Visual Relation Detection: Visual relation detection received a huge boost by the availability of large corpora of annotated datasets such as Visual Relation Detection (VRD) [Lu *et al.*, 2016] and the VG [Krishna *et al.*, 2017], containing the visual form of entities, and relations. In VRD, Word2Vec representations of the subject, object, and the predicate were used to train a model jointly with the corresponding image section describing the predicate. In particular, they consider the joint bounding box of subject and object as the image representation for the predicate. Follow-up work achieved improved performance by incorporating a knowledge graph, constructed from the image annotations [Baier *et al.*, 2017]. Later, VTransE employed TransE [Bordes *et al.*, 2013] to model visual relations. More recently, [Yu *et al.*, 2017] proposed a teacher-student model to distill external language knowledge to improve visual relation detection. Iterative Message Passing [Xu *et al.*, 2017], Neural Motifs [Zellers *et al.*, 2018] (NM) and Graph R-CNN [Yang *et al.*, 2018b] incorporate context within each prediction using RNNs and graph convolutions respectively.

Depth Maps: While several works have leveraged depth maps to improve object detection [Bo *et al.*, 2013; Eitel *et al.*, 2015; Gupta *et al.*, 2014], the idea of using depth maps in the relation detection task has only been explored in a recent work [Yang *et al.*, 2018a]. This work employs a basic framework with a handcrafted feature extractor (computing mean and mode from each depth map). The details of the architecture in this work is not clearly described. Furthermore, for evaluations they only consider human-centered relations with limited experimental settings.

3 Framework

In this section we introduce the general framework employed for this study. Let $\mathcal{E} = \{e_1, e_2, \dots, e_n\}$ be the set of all entities, including subjects (s) and objects (o), and $\mathcal{P} = \{p_1, p_2, \dots, p_m\}$ the set of all predicates. Each entity e_i can appear in images within a bounding box $bb_i = (x_i, y_i, w_i, h_i)$, where (x_i, y_i) are the coordinates of the bounding box and (w_i, h_i) are its width and height. In this work we apply Faster R-CNN [Ren *et al.*, 2015], pre-trained on ImageNet [Russakovsky *et al.*, 2015] and fine-tuned (on VG), on each image

I to extract a feature map \mathbf{fmap}_I , together with object proposals as a set of bounding boxes bb and class probability distributions c . For each RGB image, we generate a depth map D where the same bounding box areas encompass the entities’ distance from the camera. In the next section, we first describe the employed network for synthetic generation of D s and then discuss the extraction of depth features. In the end, we describe the relation detection head of the network where the late fusion of pairwise features and their relational modeling takes place.

3.1 Depth Maps for Relation Detection

Generation

We incorporate an RGB-to-Depth model within our visual relation detection framework. As shown in Figure 2, this is a fully convolutional neural network (CNN) that takes an RGB image as input and generates its predicted depth map. This model can be pre-trained on any datasets containing pairs of RGB and depth maps regardless of having the object or predicate annotations. This enables us to work with currently available visual relation detection datasets without requiring to collect additional data, and also mitigates the need for specialized hardware in real-world applications. The architectural details are explained in Section 4 and the generated depth maps from VG are separately released as a dataset called *VG-Depth*.

Feature Extraction

Depth maps have been employed in tasks such as *object detection* and *segmentation* [Eitel *et al.*, 2015; Hazirbas *et al.*, 2016]. In those works, it is common to simply render a depth map as an RGB image and extract depth features using a CNN pre-trained for RGB images. There, it has been argued that the edges in depth maps might yield better object contours than the edges in cluttered RGB images and that one may combine edges from both RGB and depth to obtain more information [Hazirbas *et al.*, 2016]. Therefore, they aimed to get similar, complementary features from both modalities. However, the practice of employing a model pre-trained on a particular source modality, e.g. RGB, and applying it on a different target modality, e.g. depth map, is sub-optimal in many applications (one should also keep in mind that even fine-tuning some layers of a network does not change the very early convolutional filters). Hence, unlike other works, we train a feature extractor CNN directly on depth maps and specifically for the task of relation detection. Given a depth map D , this network generates a feature map \mathbf{fmap}_D .

3.2 Relation Model

In the previous section, we described methods for the extraction of \mathbf{fmap}_I , \mathbf{fmap}_D , c and bb . Here, we outline the model that infers relations using pairwise combinations of these features. For each pair of detected objects within an image, we create a scale-invariant location feature $\mathbf{l}_s = (t_x, t_y, t_w, t_h)$ with: $t_x = (x_s - x_o)/w_o$, $t_y = (y_s - y_o)/h_o$, $t_w = \log(w_s/w_o)$, $t_h = \log(h_s/h_o)$ and similarly \mathbf{l}_o . We then pool the corresponding features \mathbf{v}_s and \mathbf{v}_o from \mathbf{fmap}_I and create a visual feature vector $[\mathbf{v}_s; \mathbf{v}_o]$. Similarly, we create a depth feature vector $[\mathbf{d}_s; \mathbf{d}_o]$, by pooling bb_s and bb_o from \mathbf{fmap}_D .

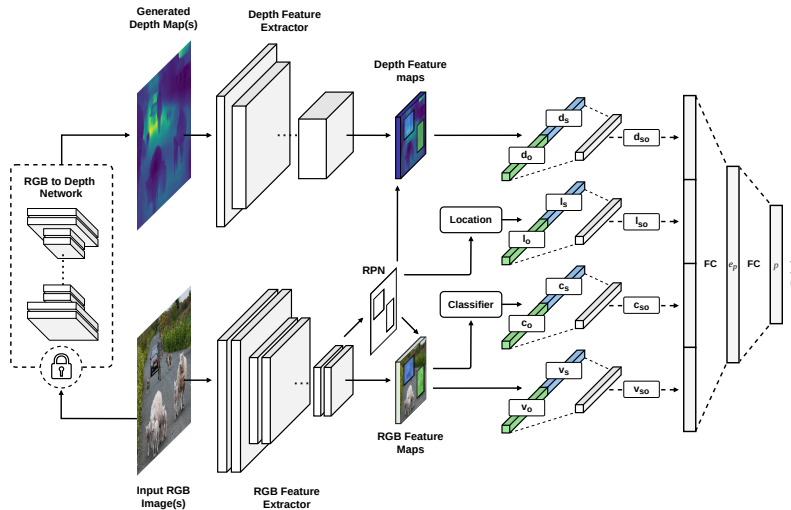


Figure 2: We study the effect of object information, i.e. class labels, location vectors, RGB and depth features in visual relation detection by employing the simple yet effective framework presented in this figure. We generate depth maps synthetically using an RGB-to-Depth model, eliminating the need of specialized hardware. On the left side, we see the RGB image and its depth map, fed into CNNs to extract feature maps from both modalities. We create pairwise feature vectors \mathbf{d}_{so} (pooled from depth feature maps), \mathbf{l}_{so} (from bounding boxes), \mathbf{c}_{so} (from class labels) and \mathbf{v}_{so} (pooled from RGB features) and feed them into a relation detection layer to infer the predicate.

Additionally, we create $[\mathbf{c}_s; \mathbf{c}_o]$ and $[\mathbf{l}_s; \mathbf{l}_o]$. Each of these vectors are fed into separate fully connected layers, yielding \mathbf{v}_{so} , \mathbf{l}_{so} , \mathbf{c}_{so} and \mathbf{d}_{so} before being fed to the relation head which projects them to the relation space such that:

$$\mathbf{e}_p = f(\mathbf{W}[\mathbf{v}_{so}; \mathbf{l}_{so}; \mathbf{c}_{so}; \mathbf{d}_{so}]). \quad (1)$$

Here, \mathbf{W} describes a linear transformation and f is a non-linear function. We realize this as a fully connected layer in a neural network with ReLU activations and dropout. \mathbf{e}_p is the embedding vector for predicate. This simple relation prediction model is inspired by the work of [Dong *et al.*, 2014] to predict links in knowledge graphs. The input of their proposed model is a triple and the output is a single Bernoulli variable, whereas in our work the inputs are *subject* and *object* and we have in output, a Bernoulli variable for each predicate class. This gives us fewer parameters compared to that model, and simplifies training by imposing an implicit negative sampling.

As shown in earlier works, using more sophisticated models for context propagation between objects with RNNs or graph convolutions, can further improve the prediction accuracy. However, the aim here is to study the effect of including depth maps as additional object features in visual relation detection and as will be shown later, even with this simple model, utilizing depth maps can be more effective than e.g. propagating context. Clearly, those other models can also further enrich their understanding of object relations by employing depth maps.

To learn the parameters, we consider each relation (s, p, o) with an associated Bernoulli variable that takes 1 if the triple is observed and 0 otherwise, following a locally closed world assumption [Nickel *et al.*, 2016]. Given the set of observed triples T , the loss function is the categorical cross entropy between the one-hot targets and the distribution obtained by

softmax over the network’s output defined as:

$$\mathcal{L} = \sum_{(s,p,o) \in T} -\log \frac{\exp(\mathbf{w}_p^T f(\mathbf{W}[\mathbf{v}_{so}; \mathbf{l}_{so}; \mathbf{c}_{so}; \mathbf{d}_{so}]))}{\sum_{p' \in \mathcal{P}} \exp(\mathbf{w}_{p'}^T f(\mathbf{W}[\mathbf{v}_{so}; \mathbf{l}_{so}; \mathbf{c}_{so}; \mathbf{d}_{so}]))} \quad (2)$$

where \mathbf{w}_p is the weight vector corresponding to p in the last layer (linear classification layer).

4 Evaluation

In our study, we are interested to answer the following questions:

1. If we are given *only* depth maps of some objects in a scene (and not even object labels), how accurately can we infer the distribution of possible pairwise relations? How do other sources of object information compare to it?
2. Current visual relation detection frameworks commonly rely on extensive object information such as class labels, bounding boxes, RGB features, contextual information, etc. Does it bring any additional information, if we also include depth representations in these frameworks or would that only contribute redundant scene knowledge?
3. Does Recall@K sufficiently reflect the improvements of under-represented relations within a highly imbalanced dataset such as VG?

In what follows, we introduce the dataset, metrics, architectural details and experiments to answer these questions.

4.1 Dataset

We test our approach on the *Visual Genome* [Krishna *et al.*, 2017] dataset. We use the more commonly used subset of VG dataset proposed by [Xu *et al.*, 2017] which contains 150 object classes and 50 relations with 75,651 images used for training, 5000 for validation and 32,422 images for testing.

Table 1: Predicate prediction recall values on VG test set. When the depth maps are utilized together with all other features (*Ours-l, c, v, d*), we gain a large improvement compared to the state-of-the-art. One can also see that even replacing depth maps with visual features (*Ours-l, c, d* compared to *Ours-l, c, v*) can yield better results. Additionally, comparing *Ours-l, c, v* to *VTransE* and *Neural Motifs* reveals the advantage of our simple model regardless of depth maps.

Strategy Task Metric	Macro			Micro			
	Predicate Pred.			Predicate Pred.			
	R@100	R@50	R@20	R@100	R@50	R@20	
models	VTransE [Zhang <i>et al.</i> , 2017]	-	-	-	62.87	62.63	-
	Yu's-S [Yu <i>et al.</i> , 2017]	-	-	-	49.88	-	-
	Yu's-S+T [Yu <i>et al.</i> , 2017]	-	-	-	55.89	-	-
	IMP [Xu <i>et al.</i> , 2017]	-	-	-	53.00	44.80	-
	Graph R-CNN [Yang <i>et al.</i> , 2018b]	-	-	-	59.10	54.20	-
	NM [Zellers <i>et al.</i> , 2018]	14.39	13.20	10.25	67.10	65.20	58.50
ablations	Ours - <i>d</i>	9.51	8.46	6.35	54.72	51.90	43.86
	Ours - <i>c</i>	15.65	13.09	8.56	64.82	60.54	49.89
	Ours - <i>v</i>	13.88	12.24	8.99	61.72	58.50	50.41
	Ours - <i>l</i>	5.19	4.66	3.57	49.07	46.13	37.48
	Ours - <i>v, d</i>	15.47	14.04	10.83	62.88	60.52	53.07
	Ours - <i>l, v, d</i>	15.76	14.40	11.07	63.06	60.83	53.55
	Ours - <i>l, c, d</i>	21.67	19.56	15.12	67.97	66.09	59.13
	Ours - <i>l, c, v</i>	19.16	17.72	13.93	67.94	66.06	59.14
	Ours - <i>l, c, v, d</i>	22.72	20.74	16.40	68.00	66.18	59.44

4.2 Metrics

Micro Recall@K: This metric is defined as the mean ratio of ground truth labels in each image that appear in the model's top K predictions and is typically called *Recall@K*. The added "Micro" prefix is to distinguish this metric with *Macro Recall@K*. Recall@K is a popular choice in most of the related visual relation detection studies. The main reason is the incompleteness of visual relation detection datasets, i.e. some relations might not be annotated in the test set, while due to the model's generalization, they might get higher prediction values than the annotated ones. This sensitivity is handled by the K parameter in Recall@K.

Macro Recall@K: This metric is defined as:

$$\text{MACRO RECALL@K} = \frac{\sum_{c \in \mathcal{C}} \text{MICRO RECALL@K}_c}{|\mathcal{C}|} \quad (3)$$

where \mathcal{C} is set of all class labels and MICRO RECALL@K_c is computed only for class label c . The motivation behind this metric is the highly imbalanced distribution of classes in some datasets such as VG. In these datasets Micro Recall@K score gets dominated by frequently labeled relations and might not reflect the improvements in some important but under-represented classes. However, in Macro R@K, the prediction accuracy of under-represented classes can have a stronger effect on the output. This metric is inspired by Macro F1 measure [Schütze *et al.*, 2008].

4.3 Architectures

RGB-to-Depth Network: We use the RGB-to-Depth model architecture introduced in [Laina *et al.*, 2016] which is a fully convolutional neural network built on ResNet-50 [He *et al.*, 2015], and trained in an end-to-end fashion on data from NYU Depth Dataset v2 [Nathan Silberman and Fergus, 2012]. Training on the outdoor images from Make3D dataset [Saxena *et al.*, 2007] instead, did not show promising results in our framework. This observation is not surprising since Make3D images contain mostly outdoor scenes with too few objects.

RGB Feature Extraction: To extract embeddings and class probabilities of RGB images, we use the VGG-16 architecture [Simonyan and Zisserman, 2014] pre-trained on ImageNet [Russakovsky *et al.*, 2015] and fine-tuned to our data for relation detection.

Depth Map Feature Extraction: For depth map extraction we use ResNet18 proposed in [He *et al.*, 2015]. We trained this model from scratch following the earlier discussions in Subsection 3.1. We trained this network on a pure depth-based, relation detection task using Adam [Kingma and Ba, 2014], with a learning rate of 10^{-4} and batch size of 32 for eight epochs.

Relation Detection Network: Finally, given the features extracted from previous models with the location features described in Subsection 3.1, we trained our relation detection model. We give each feature pair described in the previous section, separately to a fully connected hidden layer of 64, 200, 4096 and 20 neurons each, with a dropout rate of 0.1, 0.8, 0.8 and 0.1, with a scaling layer initialized as 1.0, 0.3, 0.5 and 1.0. The penultimate layer contains 4096 neurons with 0.2 dropout. We trained this network by Adam [Kingma and Ba, 2014], with a learning rate of 10^{-4} . We used a batch size of 16 and eight epochs of training. All of the layers were initialized with Xavier weights [Glorot and Bengio, 2010].

4.4 Comparing Methods

We compare our results with *VTransE* [Zhang *et al.*, 2017] that takes visual embeddings and projects them to relation space using TransE. We also compare to the student network of [Yu *et al.*, 2017] (*Yu's-S*), and their full model (*Yu's-S+T*) that employs external language data from Wikipedia. In the context propagating methods we report Neural Motifs [Zellers *et al.*, 2018], Graph R-CNN [Yang *et al.*, 2018b] and IMP [Xu *et al.*, 2017]. In an ablation study, we report our relation prediction results under several settings in which different combinations of object information are employed for prediction.

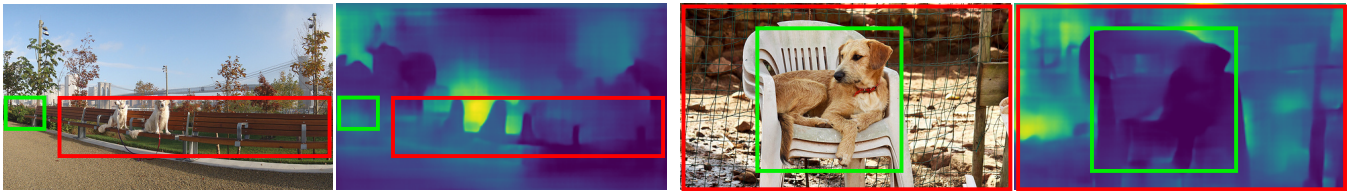


Figure 3: Using depth maps improves the understanding of *perspective* and increases the general detection rate of relations such as *behind* (e.g. right image). However, in some cases such as in the left image, after including depth maps, (*bushes, behind, bench*) has been mislabeled. One should note that here the bushes (left corner of the image) have similar depth values as the benches. Equal depth values can be a strong indicator of the predicate *next to* rather than *behind*. In this case, the human point of view seems to have caused a labelling error recovered by the depth-based model.

4.5 Experiments

As our main goal is to investigate the role of depth maps and other features in relation detection, we do not focus on improving the object detection accuracy and report *predicate prediction* results. In this setting, the relation detection performance is isolated from the object detector’s error by using ground truth bounding boxes of the entities and their class labels to predict the most likely predicates. We carried on our experiments by training each model 8 times with different random seeds. The maximum variance of the results was no more than 0.01. In the following we provide a discussion over the quantitative and qualitative results.

The complete predicate prediction results are shown in Table 1. The upper part of the table demonstrates the results directly reported from other works while the lower two parts present the results from the ablation study on our model. For NM, we have computed the Macro R@K results from their available model and code (reproducing the same Micro R@K results as reported in their paper). We can see that our full model achieves the highest accuracy in comparison to the others in all settings specially under Macro R@K. It is also interesting to note that when using *only* depth maps we can already achieve a significant accuracy in predicate prediction, emphasizing the value of relational information stored within depth maps. We can observe the improvements that depth maps bring, comparing *Ours-v* to *Ours-v, d*. Also comparing *Ours-l, c, d* to *Ours-l, c, v* is specially informative from two aspects: (1) It shows that while some results are almost equal in Micro settings, one can observe a significant difference under Macro settings, demonstrating its effectiveness in evaluating under-represented classes. (2) Considering that *v* alone has a better R@K than *d* alone when adding them separately to *c, l* we can see that *d* has more to offer. In other words, *v* has more redundant information for *c, l* compared to *d*.

To get a better intuition of the improvements that we gain after including depth maps (*Ours-v, d* compared to *Ours-v*), we plotted the changes in prediction accuracy for each predicate in Figure 4. We used darker shades for over-represented classes and lighter shades for under-represented ones. This helps to also gain a better intuition of improvement versus representativeness. For example we can see that in general the accuracy of relations including the predicates such as *under, in front of* and *behind* has been improved.

In our qualitative studies, we also observed that in some cases the predicate *behind* was mislabeled after adding the

depth maps. To further explore the potential reasons behind such failures, we further examined the test images. Figure 3 gives an example of a failure and a success case in predicting *behind*. While in the right image the annotations indicate that (*bushes, behind, bench*) based on the corresponding depth map, they are in the same distance from the camera. One can argue that in fact, bushes are next to the bench rather than behind, indicating the noisy ground truth. However, it is also important to note that humans describe a predicate from their inner point of view which is not necessarily associated with the camera’s point of view. This effect might appear in many other instances within the dataset, leading to worse performances when dealing with such predicates. A simple way to overcome such problems is by having a richer dataset.

We provide some samples of high and lower quality depth maps generated from VG images in Figure 5.

5 Conclusion

We employed an RGB-to-Depth network, trained on a large corpus of data, to generate depth maps for Visual Genome dataset, releasing a new extension called *VG-Depth*. We provided a metric, *Macro R@K* for better evaluation of relation detection in Visual Genome and other highly imbalanced datasets. In extensive empirical evaluations, we demonstrated the effect of different object information in visual relation detection and showed that by using depth information, one achieves significantly better performance compared to other state-of-the-art methods.

References

- [Baier *et al.*, 2017] Stephan Baier, Yunpu Ma, and Volker Tresp. Improving visual relationship detection using semantic modeling of scene descriptions. In *International Semantic Web Conference*, pages 53–68. Springer, 2017.
- [Bo *et al.*, 2013] Liefeng Bo, Xiaofeng Ren, and Dieter Fox. Unsupervised feature learning for rgb-d based object recognition. In *Experimental Robotics*, pages 387–402. Springer, 2013.
- [Bordes *et al.*, 2013] Antoine Bordes, Nicolas Usunier, Alberto Garcia-Duran, Jason Weston, and Oksana Yakhnenko. Translating embeddings for modeling multi-relational data. In *Advances in neural information processing systems*, pages 2787–2795, 2013.

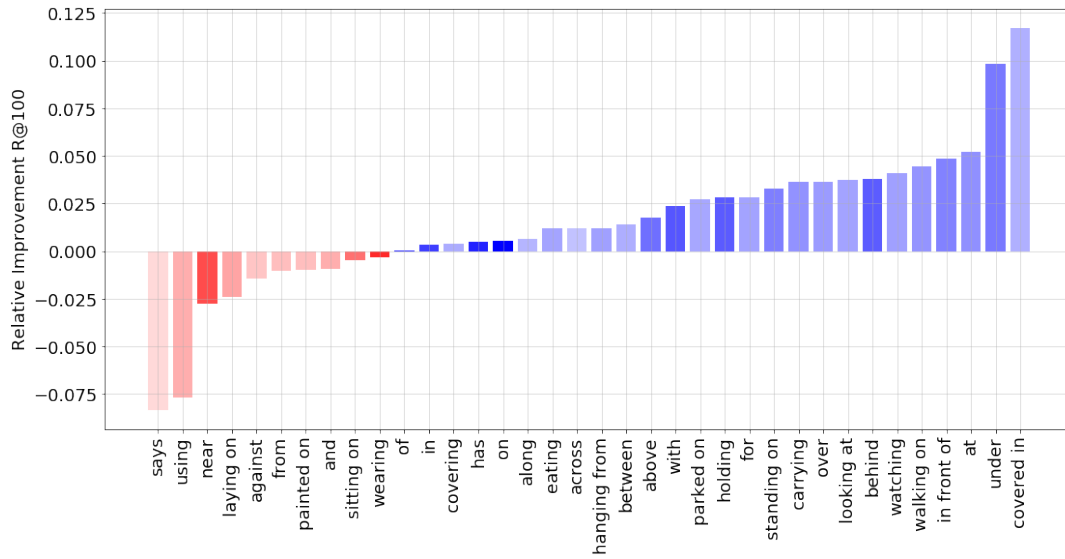


Figure 4: This plot shows the prediction changes per predicate, going from *Ours-v* to *Ours-v, d*. The classes with zero changes are omitted from the plot. The darker shades indicate larger number of that class within the test set whereas the lighter shades are under-represented classes. An improvement in predicates with more frequency has a larger effect on the Micro R@K whereas this effect is eliminated within Macro R@K. We can see that indeed the improvements by using depth maps are mostly happening within the less-represented classes.

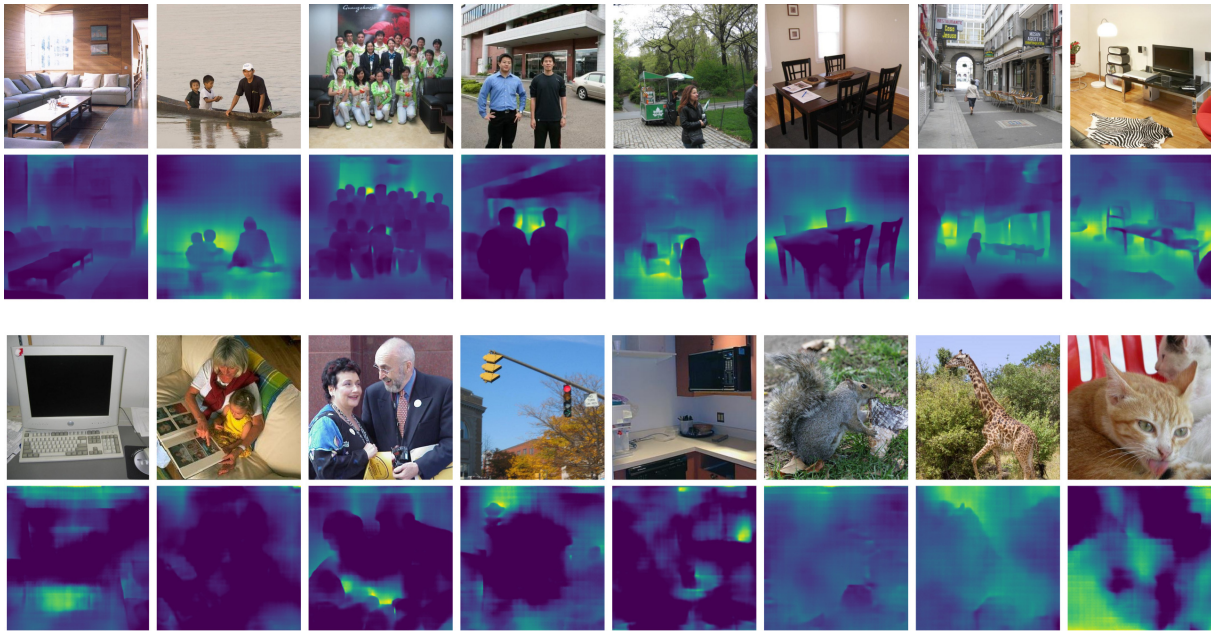


Figure 5: The first two rows are the examples of visual genome images and their synthetically generated high quality depth maps. The second two rows are the examples of visual genome images and their synthetically generated lower quality depth maps.

- [Dong *et al.*, 2014] Xin Dong, Evgeniy Gabrilovich, Jeremy Heitz, Wilko Horn, Ni Lao, Kevin Murphy, Thomas Strohmann, Shaohua Sun, and Wei Zhang. Knowledge vault: A web-scale approach to probabilistic knowledge fusion. In *Proceedings of the 20th ACM SIGKDD international conference on Knowledge discovery and data mining*, pages 601–610. ACM, 2014.
- [Eitel *et al.*, 2015] Andreas Eitel, Jost Tobias Springenberg, Luciano Spinello, Martin Riedmiller, and Wolfram Burgard. Multimodal deep learning for robust rgb-d object recognition. In *Intelligent Robots and Systems (IROS), 2015 IEEE/RSJ International Conference on*, pages 681–687. IEEE, 2015.
- [Glorot and Bengio, 2010] Xavier Glorot and Yoshua Bengio. Understanding the difficulty of training deep feedforward neural networks. In *Proceedings of the thirteenth international conference on artificial intelligence and statistics*, pages 249–256, 2010.
- [Gupta *et al.*, 2014] Saurabh Gupta, Ross Girshick, Pablo Arbeláez, and Jitendra Malik. Learning rich features from rgb-d images for object detection and segmentation. In *European Conference on Computer Vision*, pages 345–360. Springer, 2014.
- [Hazirbas *et al.*, 2016] Caner Hazirbas, Lingni Ma, Csaba Domokos, and Daniel Cremers. Fusetnet: Incorporating depth into semantic segmentation via fusion-based cnn architecture. In *Asian Conference on Computer Vision*, pages 213–228. Springer, 2016.
- [He *et al.*, 2015] Kaiming He, Xiangyu Zhang, Shaoqing Ren, and Jian Sun. Deep residual learning for image recognition. *CoRR*, abs/1512.03385, 2015.
- [Kingma and Ba, 2014] Diederik P Kingma and Jimmy Ba. Adam: A method for stochastic optimization. *arXiv preprint arXiv:1412.6980*, 2014.
- [Krishna *et al.*, 2017] Ranjay Krishna, Yuke Zhu, Oliver Groth, Justin Johnson, Kenji Hata, Joshua Kravitz, Stephanie Chen, Yannis Kalantidis, Li-Jia Li, David A Shamma, et al. Visual genome: Connecting language and vision using crowdsourced dense image annotations. *International Journal of Computer Vision*, 123(1):32–73, 2017.
- [Laina *et al.*, 2016] Iro Laina, Christian Rupprecht, Vasileios Belagiannis, Federico Tombari, and Nassir Navab. Deeper depth prediction with fully convolutional residual networks. In *3D Vision (3DV), 2016 Fourth International Conference on*, pages 239–248. IEEE, 2016.
- [Lu *et al.*, 2016] Cewu Lu, Ranjay Krishna, Michael Bernstein, and Li Fei-Fei. Visual relationship detection with language priors. In *European Conference on Computer Vision*, pages 852–869. Springer, 2016.
- [Nathan Silberman and Fergus, 2012] Pushmeet Kohli Nathan Silberman, Derek Hoiem and Rob Fergus. Indoor segmentation and support inference from rgb-d images. In *ECCV*, 2012.
- [Nickel *et al.*, 2016] Maximilian Nickel, Kevin Murphy, Volker Tresp, and Evgeniy Gabrilovich. A review of relational machine learning for knowledge graphs. *Proceedings of the IEEE*, 104(1):11–33, 2016.
- [Ren *et al.*, 2015] Shaoqing Ren, Kaiming He, Ross Girshick, and Jian Sun. Faster r-cnn: Towards real-time object detection with region proposal networks. In *Advances in neural information processing systems*, pages 91–99, 2015.
- [Russakovsky *et al.*, 2015] Olga Russakovsky, Jia Deng, Hao Su, Jonathan Krause, Sanjeev Satheesh, Sean Ma, Zhiheng Huang, Andrej Karpathy, Aditya Khosla, Michael Bernstein, Alexander C. Berg, and Li Fei-Fei. ImageNet Large Scale Visual Recognition Challenge. *International Journal of Computer Vision (IJCV)*, 115(3):211–252, 2015.
- [Saxena *et al.*, 2007] Ashutosh Saxena, Min Sun, and Andrew Y Ng. Learning 3-d scene structure from a single still image. In *Computer Vision, 2007. ICCV 2007. IEEE 11th International Conference on*, pages 1–8. IEEE, 2007.
- [Schütze *et al.*, 2008] Hinrich Schütze, Christopher D Manning, and Prabhakar Raghavan. Introduction to information retrieval. In *Proceedings of the international communication of association for computing machinery conference*, page 260, 2008.
- [Simonyan and Zisserman, 2014] Karen Simonyan and Andrew Zisserman. Very deep convolutional networks for large-scale image recognition. *arXiv preprint arXiv:1409.1556*, 2014.
- [Xu *et al.*, 2017] Danfei Xu, Yuke Zhu, Christopher B Choy, and Li Fei-Fei. Scene graph generation by iterative message passing. In *Proceedings of the IEEE Conference on Computer Vision and Pattern Recognition*, pages 5410–5419, 2017.
- [Yang *et al.*, 2018a] Hsuan-Kung Yang, An-Chieh Cheng, Kuan-Wei Ho, Tsu-Jui Fu, and Chun-Yi Lee. Visual relationship prediction via label clustering and incorporation of depth information. In *Proceedings of the European Conference on Computer Vision (ECCV)*, pages 0–0, 2018.
- [Yang *et al.*, 2018b] Jianwei Yang, Jiasen Lu, Stefan Lee, Dhruv Batra, and Devi Parikh. Graph r-cnn for scene graph generation. In *Proceedings of the European Conference on Computer Vision (ECCV)*, pages 670–685, 2018.
- [Yu *et al.*, 2017] Ruichi Yu, Ang Li, Vlad I Morariu, and Larry S Davis. Visual relationship detection with internal and external linguistic knowledge distillation. In *IEEE International Conference on Computer Vision (ICCV)*, 2017.
- [Zellers *et al.*, 2018] Rowan Zellers, Mark Yatskar, Sam Thomson, and Yejin Choi. Neural motifs: Scene graph parsing with global context. In *Proceedings of the IEEE Conference on Computer Vision and Pattern Recognition*, pages 5831–5840, 2018.
- [Zhang *et al.*, 2017] Hanwang Zhang, Zawlin Kyaw, Shih-Fu Chang, and Tat-Seng Chua. Visual translation embedding network for visual relation detection. In *2017 IEEE Conference on Computer Vision and Pattern Recognition, CVPR 2017, Honolulu, HI, USA, July 21-26, 2017*, pages 3107–3115. IEEE Computer Society, 2017.